Open Access

Recent Progress in Science and Engineering

LIDSEN Publishing Inc.

Original Research

Utilising Ethanol Extract of the Leaves of African Peach for Corrosion Protection of Mild Steel in 1.0 M NaOH: Electrochemical and Gravimetric Assessments

Matthew A. Adebayo *, O'Seun Odewale, Olabisi A. Ajayi

Department of Chemistry, The Federal University of Technology, Akure, Nigeria; E-Mails: adebayoma@futa.edu.ng; oodewale@me.com; ajayiolabisi@futa.edu.ng

* **Correspondence:** Matthew A. Adebayo; E-Mail: adebayoma@futa.edu.ng

Academic Editor: Ali Asghar Javidparvar

Special Issue: Corrosion Characterization and Sustainable Protection in Advanced Materials

Recent Prog Sci Eng
2026, volume 2, issue 2
doi:10.21926/rpse.2602012

Received: April 03, 2026
Accepted: June 21, 2026
Published: June 29, 2026

Abstract

Mild steel tends to form a protective film in caustic environments; however, elevated temperatures and freshly exposed metal surfaces usually prevent stable film formation—leading to a rapid and active corrosion rate. This study reports the potential of the ethanol extract of African peach (*Nauclea latifolia*) leaf as an alternative corrosion inhibitor of mild steel in 1.0 M NaOH solution. Gravimetric and electrochemical measurements were carried out to unravel the mechanisms of the corrosion reduction by the inhibitor, while Scanning Electron Microscopy (SEM) and Energy Dispersive X-ray (EDX) spectroscopy were used to visualise the surface structures and relative elemental compositions of the inhibitor, mild steel, and mild steel after immersion in inhibited solution (1.0 M NaOH + inhibitor). Equilibrium data were subjected to Langmuir, Freundlich, and Temkin models, while the temperature-dependent data were analysed using appropriate thermodynamic equations. The correction rate declined marginally with increasing inhibitor concentration, whereas the inhibition efficiency increased substantially. Variations in experimental temperature had a minimal effect on the inhibition efficiency of the inhibitor in protecting the mild steel surface. The equilibrium data obeyed the Langmuir isotherm model. The adsorption of the inhibitor onto

the mild steel surface was spontaneous, involving physisorption, and was endothermic. The observed reduction in corrosion current density (I_{corr}) and the corresponding increase in inhibition efficiency from polarisation measurements, alongside the significantly enhanced charge transfer resistance (R_{ct}) derived from Electrochemical Impedance Spectroscopy (EIS), collectively confirm the effective corrosion inhibition performance of the African peach extract through a diffusion-controlled adsorption mechanism. Hence, *Nauclea latifolia* leaf extract could serve as a viable, alternative, and eco-friendly corrosion inhibitor for mild steel in alkaline environments.

Keywords
African peach leaves; corrosion inhibitor; mild steel; gravimetric analysis; electrochemical study; sodium hydroxide

1. Introduction

The corrosion process is a gradual deterioration and degradation of a metal's surface as a result of its chemical and electrochemical interactions with the environment [1]. This process causes safety concerns due to material failure and economic losses. The corrosion process affects industrial development across many sectors, including construction, transportation, oil and gas, manufacturing, power generation, mining and mineral processing, military and defense, among others. There is a need to implement an effective strategy for corrosion control and prevention to reduce economic damage from metal corrosion [2]. Nowadays, many industries are adopting advanced protective techniques such as high-performance powder coatings and the development of new materials to avoid unwanted economic loss due to corrosion of metals. Mild steel is a popular and widely used engineering material due to its good mechanical features, manufacturing versatility, excellent physical and magnetic properties, availability, and affordability [3, 4]. However, mild steel's susceptibility to corrosion in corrosive media, usually encountered during industrial processes (including acid cleaning, descaling, and pickling), affects the long-term performance of mild steel [5]. Chemical reactions with hydroxide ions and dissolved salts cause mild steel to corrode in alkaline environments, although the corrosion rate is slower than in acidic conditions. Chemicals such as NaOH, KOH, Na_2CO_3, and $Ca(OH)_2$ can attack mild steel surfaces in concrete reinforcements, caustic soda vats, power plant cooling systems, and pulping liquor tanks [6]. Alkaline media are used in industries such as chemical processing, petroleum refining, textile manufacturing, soap and detergent, water treatment, and so on. Exposure of mild steel to concentrated NaOH can render it susceptible to corrosion, cracking, and surface degradation [7]. As a result, the usage of corrosion inhibitors has become a cost-saving and practical method for the mitigation of mild steel deterioration.

A corrosion inhibitor is a substance that, when added in minute amounts to corrosive media, reduces the corrosion rate or inhibits the corrosion of a material, typically a metal or an alloy that is exposed to the fluid [8]. A corrosion inhibitor protects a metal's surface from corrosion, and the effectiveness of a corrosion inhibitor depends on the composition of the fluid, the quantity of water, and the flow regime [9]. Inhibitors function by either promoting the oxidation of the metal to form

an impervious layer, otherwise known as passivation (inorganic inhibitors), or by adsorbing onto the metal surface through their heteroatoms or multiple bonds (organic inhibitors). This adsorption forms a hydrophobic layer that hinders aggressive agents present in the environment from gaining access to the metal's surface. Conventional (inorganic) corrosion inhibitors, which are mostly synthetic chemicals, have shown serious environmental and hazardous features due to their toxicity and non-biodegradability [10]. To comply with environmental regulations and for the safety of human lives, there has been a push towards the search for green, alternative, and sustainable industrial practices, and this has led to the development of green (mostly organic) corrosion inhibitors that are obtainable from diverse natural sources. These green inhibitors are advantageous over inorganic counterparts because they are eco-friendly, biodegradable, available, and rich in bioactive phytochemicals such as alkaloids, flavonoids, tannins, and saponins that could facilitate adsorption onto metal surfaces and form protective films against corrosion [11, 12].

Extracts of plant parts (leaves, fruits, stems, bark, roots, seeds, and peels), which are rich in bioactive phytochemicals, have emerged as green inhibitors due to their effectiveness and low negative impacts on the environment [13]. Among these alternative inhibitors, African peach {*Sacrocephalus latifolius* (Sm.) EA Bruce, also known as *Nauclea latifolia* Sm.}, leaf extract could serve as a potential corrosion inhibitor for mild steel in a harsh environment. The plant is widely distributed across tropical Africa. It is known for its rich composition of bioactive compounds, including phenolic constituents and nitrogen-containing molecules [14], which could enhance its adsorption capability on metal surfaces. These compounds have a high probability of interacting with the mild steel surface through physisorption and/or chemisorption mechanisms to reduce corrosion rates and improve inhibition efficiencies.

This study investigates the corrosion inhibition performance of African peach leaf extract on mild steel in 1.0 M NaOH. Emphasis is placed on understanding the adsorption behavior, inhibition efficiency, and surface interaction mechanisms, with the aim of contributing to the development of sustainable and environmentally friendly corrosion control strategies to reduce economic loss due to mild steel corrosion. Measurements *via* gravimetric and electrochemical experiments were carried out to probe the corrosion inhibition potential of African peach leaf extract. The novelty of this study also includes the application of a renewable, green, sustainable, biodegradable, and low-toxicity inhibitor from African peach for corrosion mitigation of mild steel in an alkaline medium, serving as an environmentally friendly alternative to synthetic inhibitors in alkaline corrosion systems.

2. Materials and Methods

2.1 Collection of Plant Leaves and Preparation of Extract

African peach leaves were collected from Iroko-Ekiti, in Ijero Local Government Area of Ekiti State, Nigeria. The leaves were authenticated at the Department of Crop, Soil and Pest Management of The Federal University of Technology, Akure, Nigeria. The leaves were washed with clean running water from a tap to remove dirt and impurities. The leaves were air-dried for 21 days, pulverized, and the pulverized sample was weighed and kept in a clean specimen container until ready for use [15, 16].

The ethanol extract of African peach dried sample was obtained by measuring 10 g of the powdered sample into a Soxhlet apparatus and extracted with ethanol (70-80°C) till a colour change

was observed. The extract solution was then collected, concentrated over a thermostatic water bath at 45°C, and stored until use.

2.2 Preparation of Coupons and Gravimetry Experiments

This study employed coupons cut from mild steel of known composition by weight percent (Fe-58.83%; Ca-0.87%; Ti-0.69%; Mg-0.59%; Mn-0.49%; Al-0.47%; Co-0.42%). The cut-out coupons with dimensions of 24 × 15 × 4 mm were polished with emery paper to remove surface particles. The dimensions of coupons for gravimetry and electrochemical studies were the same. The mild steel samples were thoroughly washed first under running water and later then with deionized water and ethanol before being dried in air [16]. The samples were stored in a desiccator afterward. A digital electronic balance was then used to take the weights of the coupons and record them in a logbook. All chemicals (solvents and reagents) used for this project were of analytical grade; they were not subjected to further treatment. In contrast, deionized water was used to prepare the samples.

Before the coupons were used for the study, they were thoroughly washed under deionized water, then ethanol, and dried with a clean handkerchief. Thereafter, the coupons were hung by thread and a glass rod in 100 ml of aqueous 1.0 M NaOH medium in a 250 ml glass beaker, containing a specific amount of ethanol extract of the African peach leaf. The concentration study was carried out by varying the concentration of the extract from 0.2 g/L to 1.0 g/L in 100 mL of separate solutions containing 1.0 M NaOH. Each coupon with known dimension and initial weight in gramme (W_1) was immersed inside the respective concentration of the blank (1.0 M NaOH) and inhibitor solution for 6 h after which it was retrieved, rinsed with distilled water (to remove corrosive residues and products) and acetone (to remove residual water, organic residues, oils, etc.), dried with clean handkerchief and re-weighed (W_2) [17]. The weight loss in gramme (g), W_3, was calculated by subtracting final weight from initial weight ($W_1 - W_2$). After gravimetric corrosion experiments, values of corrosion rates (CR_{grav}, g cm^{-2} h^{-1}) and inhibition efficiencies (IE_{grav} %) were evaluated with the aid of Equations 1 and 2, respectively.

$$CR_{grav} = \frac{w_3}{A \cdot t} \tag{1}$$

$$IE_{grav}\% = \frac{CR_b - CR_i}{CR_b} \times 100 \tag{2}$$

where A is the surface area of the coupon (cm^2); t is the immersion time (h); and CR_b and CR_i are the respective corrosion rates in the absence (blank) and presence of extract (inhibitor) at various concentrations.

To probe the effect of immersion time on the corrosion characteristics, experiments were performed at varying times (24, 48, 72, 96, 120, 144, and 168 h). Similarly, the effect of temperature on the corrosion study was investigated at 28, 40, 50, and 60°C in a thermostatic shaker. The thermodynamic and activation parameters of the reaction were evaluated using the data from the temperature study. The activation energy, E_A, was calculated using the Arrhenius equation as shown in Equation 3, while the other thermodynamic parameters (standard entropy change, ΔS°_{ads}, and standard enthalpy change of activation, ΔH°_{ads}) were calculated using Equation 4.

$$\ln CR_{grav} = \ln A - \frac{E_A}{RT} \tag{3}$$

$$\log\left(\frac{CR_{grav}}{T}\right) = \left[\log\left(\frac{R}{N \cdot h}\right) + \frac{\Delta S^{\circ}_{ads}}{2.303R}\right] - \frac{\Delta H^{\circ}_{ads}}{2.303RT} \tag{4}$$

where A is the Arrhenius pre-exponential factor, E_A is the activation energy (kJ mol^{-1}), T is the absolute temperature (K), R is the universal gas constant (J K^{-1} mol^{-1}), N is Avogadro's constant (mol^{-1}), h is Planck's constant (J s), ΔS°_{ads} is the standard change in entropy (J mol K^{-1}), and ΔH°_{ads} is the standard enthalpy of activation (kJ mol^{-1}).

The concentration dependent (equilibrium) data were subjected to Langmuir, Freundlich and Temkin models which are represented in Equations 5-7, respectively.

$$\frac{C}{\theta} = \frac{1}{K_L} + C \tag{5}$$

$$\log\theta = \log K_F + \frac{1}{n_F}\log C \tag{6}$$

$$\theta = -\frac{\ln K_T}{2a} - \frac{\ln C}{2a} \tag{7}$$

where ϑ = fractional surface coverage; C = concentration of the inhibitor; K_F, K_L and K_T = Langmuir, Freundlich and Temkin equilibrium constants, respectively, n_F = Freundlich empirical constant, and a = interaction parameter.

2.3 Electrochemical Corrosion Study

Potentiodynamic polarisation (PDP) and open circuit potential (OCP) measurements were carried out using the electrochemical impedance spectrophotometry (EIS) technique at 28°C. The details of electrochemical studies followed our earlier procedure [16]. Using an ammeter connected in series, the OCP measurements were carried out at different cathodic and anodic potentials with varying concentrations of African peach leaf extract applied on the WE (working electrode) in the range ±250 mV at a scan rate of 1.0 mV s^{-1} for 30 min to obtain the current densities.

The corrosion inhibition efficiency (IE_{EIS} %) was calculated from EIS data using Equation 8 while corrosion rate (CR_{PDP}) and IE_{PDP} % were also calculated from PDP using respective Equations 9 and 10, respectively.

$$IE_{EIS}\% = \left(1 - \frac{R^0_{ct}}{R_{ct}}\right) \times 100 \tag{8}$$

$$CR_{PDP} = \frac{k \cdot I_{corr} \cdot EW}{\rho} \tag{9}$$

$$IE_{PDP}\% = \left(\frac{I_{corr} - I_{corr_{inh}}}{I_{corr_{inh}}}\right) \times 100 \tag{10}$$

where R_{ct}^{0} and R_{ct} = respective charge transfer resistance of the uninhibited and inhibited solutions, *EW* = steel's equivalent weight, ρ = density (g cm^{-3}) of the mild steel, *k* = conversion factor (3.27 × 10^{-3}), I_{corr} and $I_{corr_{inh}}$ = respective corrosion current densities (µA cm^{-2}) without and with inhibitors.

2.4 Characterisation Study

The FTIR spectra of the samples (plant extract, mild steel, and mild steel + extract + 1.0 M NaOH) were obtained on Thermo Fischer Scientific (Nicolet iS5, iD7 ATR, Germany) to detect various functional groups in the samples. Surface examinations of the plant extract, mild steel, and mild steel specimen immersed in 1.0 M NaOH solutions in the presence of optimum concentration (1.0 g/L) of crude extract were done using SEM-EDX (Zeiss 121 DSM 982 Gemini) after 24 h of immersion time at room temperature (~28°C). The sample was removed from the solution, rinsed, dried and kept in a desiccator to prevent the formation of hydrofluoric acid, which may damage the sample and interfere with the EDX measurements. The coupons were coated with a conductive layer to prevent charging during SEM imaging.

3. Results and Discussion

Ethanol extract of African peach leaves was obtained and assessed as a corrosion inhibitor of mild steel in 1.0 M NaOH.

3.1 Gravimetry Study

Corrosion rates of mild steel and inhibition efficiencies of the inhibitors are always dependent on the concentration of inhibitors present in the corrosive media. Generally, the extracts from plants could serve as eco-friendly corrosion inhibitors, and the performance of these green inhibitors to protect metals' surfaces improves as their concentrations in corrosive media increase due to increased adsorption and protective film formation on the metals' surfaces [18]. Figure 1 presents the dependence of the corrosion rate of mild steel and the inhibition efficiency of African peach extract on the concentration of the extract (inhibitor) in 1.0 M NaOH at 28°C and 6 h. As the concentration of the inhibitor increases (from 0.2 g/L to 1.0 g/L), the corrosion rate of mild steel in the alkaline medium slightly decreases (from 9.8 × 10^{-5} to 2.6 × 10^{-5} g/cm^2 h). This observation could be linked to the presence of more phytochemical constituents that can be adsorbed on the surface of the mild steel [13]—this forms a protective film against corrosion on the surface of the metal. However, the inhibition efficiency of the inhibitor increases (from 38.7% to 73.2%) as the concentration of the inhibitor increases (from 0.2 g/L to 1.0 g/L). This is expected because at a low concentration of inhibitor, the mild steel surface in an alkaline medium was partly covered, which resulted in low to moderate protection. A high concentration of the inhibitor provided high adsorption active sites for coverage, and this resulted in improved corrosion resistance of the metal.

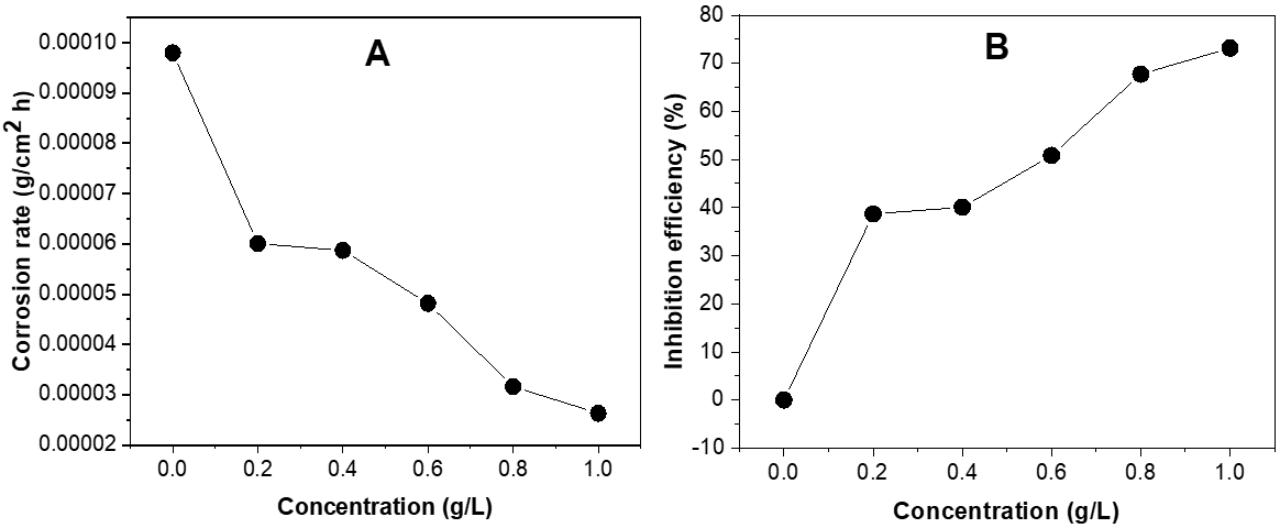

Figure 1 Effect of inhibitor concentration on corrosion rate (A) and inhibition efficiency (B).

The temperature of the corrosion system is adjudged to play a significant role in corrosion experiments, and variation in temperature mostly affects the corrosion rate of mild steel in corrosive media and the inhibition efficiency of the inhibitor [10]. Figure 2 presents the combined effects of inhibitor concentration and temperature on the corrosion rates and inhibition efficiencies. Corrosion rate significantly increased as the temperature was increased from 28°C to 40°C. There were slight changes in corrosion rates between 40 and 60°C, especially in the inhibited systems. An increase in corrosion rates as temperature increased could be related to high mass loss due to an increase in mild steel dissolution in the corrosive (1.0 M NaOH) medium [19]. The inhibition efficiency of the African peach leaf extract for mild steel protection improved with increasing concentration as the temperature of the medium was increased.

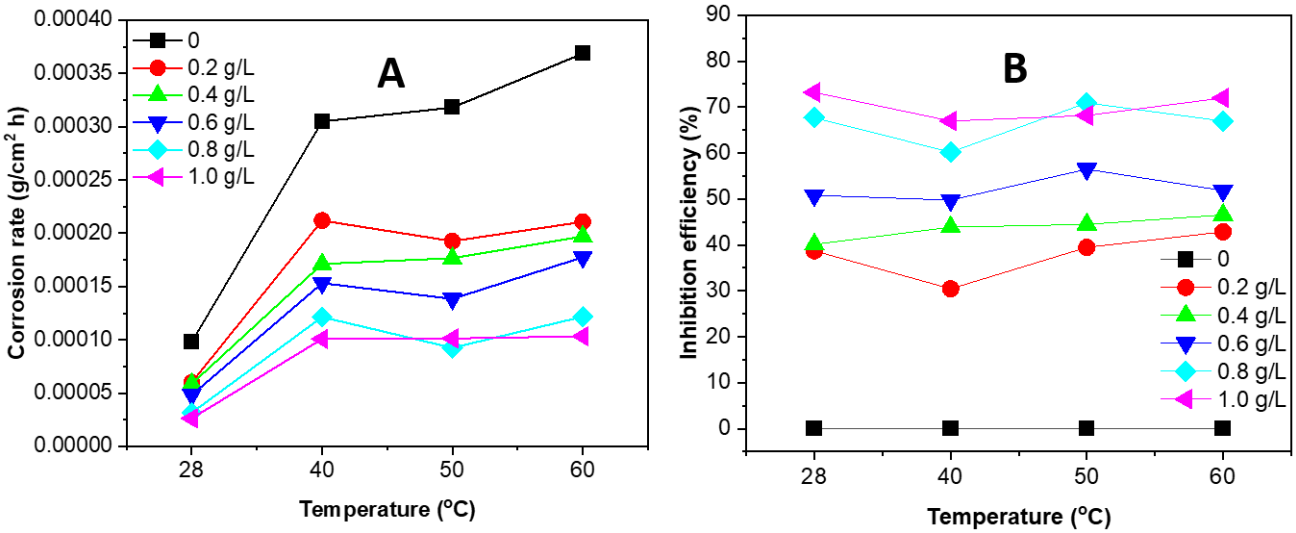

Figure 2 Effect of temperature on corrosion rate (A) and inhibition efficiency (B).

The duration of immersion in a corrosion environment provides important information about the corrosion rate. Figure 3 presents the effect of immersion time of mild steel in 1.0 M NaOH in the

absence and presence of inhibitor (over different concentration values) at 28°C. The corrosion rate was higher in the blank (uninhibited system) than in the other inhibited systems, and in general, the corrosion rate decreased as the concentration of the inhibitor was increased over the time range. It is noticeable in the figure that the corrosion rate increased as immersion time increased from 24 h to 72 h; after 72 h, the corrosion rate significantly decreased till 168 h of immersion. The observation could be linked to the scenario in which the mild steel surface is highly reactive at the initial stage of the experiment where there was no protective layer, and the 1.0 M NaOH corrosive medium attacked the mild steel surface leading to mild steel dissolution and the corresponding weight loss (high corrosion rate). However, as the immersion time was prolonged, there was the formation of a protective film on the surface of mild steel by the inhibitor, and this film formed a barrier (reduction of contact) between the mild steel surface and the alkaline medium; hence, a reduction in corrosion rate [20, 21]. For inhibited corrosion systems, there was a negligible increase in the inhibition efficiency of the inhibitor from immersion time of 24 h to 48 h; after 48 h immersion time, the corrosion efficiency slightly decreased, and this phenomenon can be linked to partial desorption of the inhibitor from the metal surface as well as degradation of inhibitor molecules, which weakened the protective film [22, 23].

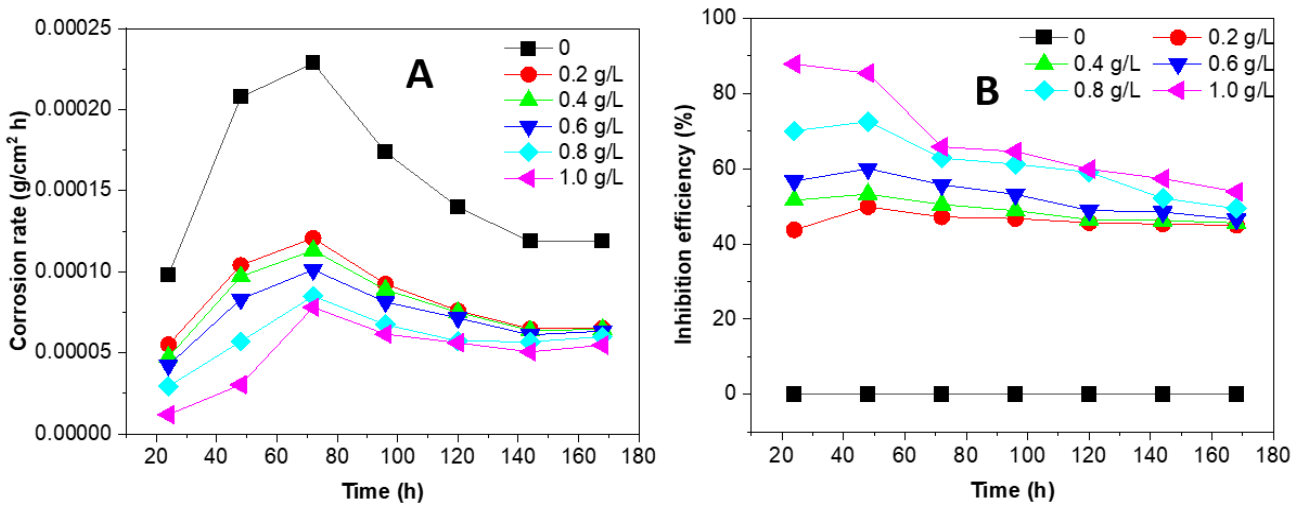

Figure 3 Effect of time on corrosion rate (A) and inhibition efficiency (B) of the inhibitor.

3.2 Adsorption Isotherms

Adsorption isotherms are usually used to describe the relation between inhibitor molecule coverage on the metal surface and inhibitor concentration in the bulk solution [24]. To deduce the mechanisms of corrosion inhibition, the values of surface coverage (ϑ), corresponding to different studied concentrations of African peach leaf extract in the selected temperature range (301 to 333 K), were tested by fitting isotherm (equilibrium) data into Langmuir, Freundlich, and Temkin adsorption models, and the plots of these models are presented in Figure 4. Table 1 presents the parameters of these models. It is evident that the Langmuir model suitably described the adsorption of the inhibitor onto the mild steel surface because this model gave the highest values of R^2_{adj} (adjusted correlation coefficient) across all the experimental temperatures. The Langmuir isotherm is a quantitative model useful for describing the adsorption of the inhibitor onto the metal surface, assuming a monolayer coverage of the inhibitor on homogeneous sites [24]. For the isotherm data

to follow the Langmuir model in this study signifies that the adsorption characteristics features are close to ideal monolayer adsorption. It implies that there was adsorption of inhibitor molecules to form a protective layer that mitigates the dissolution of mild steel. The value of K_L is ≈1 across temperatures, indicating strong interaction and high inhibition effectiveness of African peach leaf extract in preventing corrosion of mild steel [24].

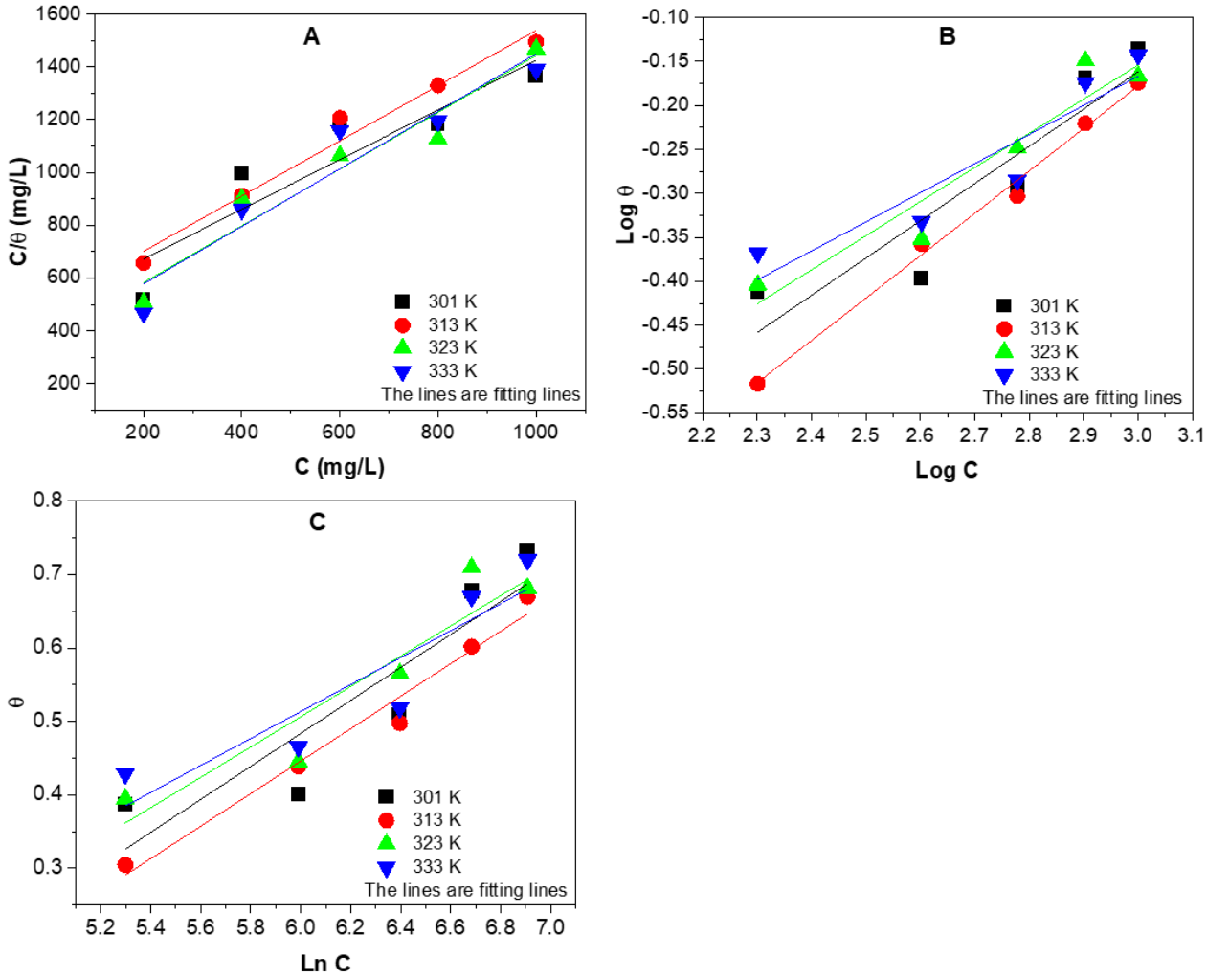

Figure 4 Langmuir (A), Freundlich (B), and Temkin (C) modeling of corrosion protection of mild steel using African peach leaf extract.

Table 1 Calculated Langmuir, Freundlich, and Temkin equilibrium parameters for mild steel corrosion protection using African peach leaf extract.

Temperature (K)		301	313	323	333
Langmuir	K_L	1.0622	0.95647	0.93072	0.91746
	R^2_{adj}	0.87803	0.99609	0.92099	0.89162
Freundlich	K_F	0.036941	0.023778	0.048045	0.069170
	n_F	2.3607	2.0749	2.5767	3.0203
	R^2_{adj}	0.79766	0.98048	0.88428	0.81860
Temkin	K_T	0.021370	0.018611	0.028922	0.040704
	A	-2.2274	-2.2612	-2.4266	-2.7257
	R^2_{adj}	0.75883	0.96594	0.84292	0.77218

3.3 Thermodynamic Characteristics of the Corrosion Systems

To probe the characteristics of the mild steel-African peach leaf extract thermodynamic system, the temperature-dependent data were subjected to thermodynamic inquisition, such as Arrhenius and Eyring equations. Arrhenius and Eyring plots are presented in Figure 5, while Table 2 and Table 3 summarize the thermodynamic parameters. As presented in Table 2, the values of standard Gibb's free energy (ΔG°_{ads}), which were calculated from Equation 11, are negative which shows that the thermodynamics of the corrosion and adsorption process is spontaneous. This observation means that there was an interaction between the molecules of African peach leaf extract and the mild steel, leading to the formation of a good protective film that reduced corrosion density. When the value of ΔG°_{ads} is *ca.* -20 kJ mol^{-1} or less negative, the process is termed physisorption (electrostatic interaction), the value of ΔG°_{ads} *ca.* -40 kJ mol^{-1} or more negative connotes chemisorption (chemical bonding) while the value of ΔG°_{ads} that lied between -20 and -40 kJ mol^{-1} represents mixed adsorption [25]. The values of ΔG°_{ads} (between -10.202 and -10.881 kJ/mol) obtained in this study over the experimental temperature range (301-333 K) indicate spontaneous physisorption of molecular extract of the African peach on mild steel coupons [15].

$$\Delta G^{\circ}_{ads} = -RT\ln(55.5 \times K_L) \tag{11}$$

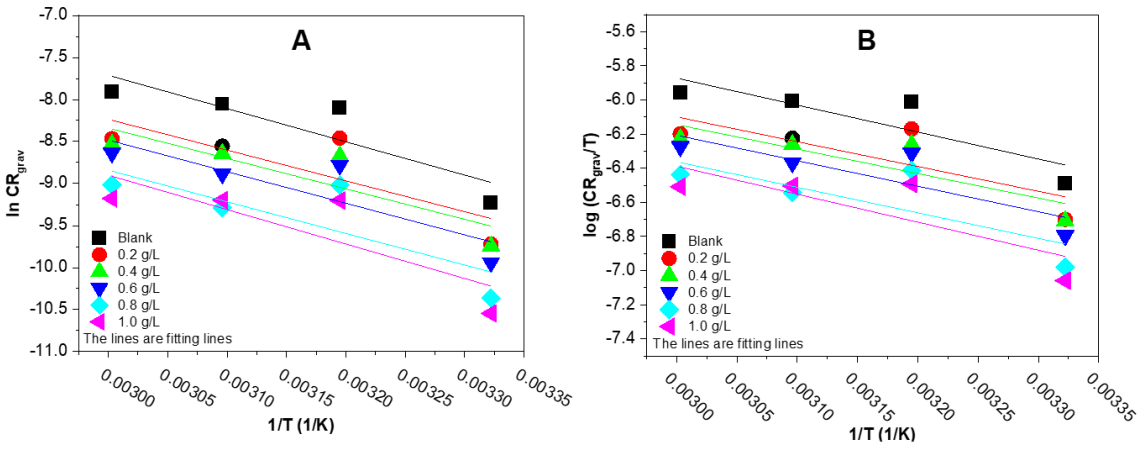

Figure 5 Arrhenius (A) and Eyring (B) plots of the adsorption of African peach leaf extract on mild steel surface in 1.0 M NaOH.

Table 2 The Gibb's energy of the corrosion process.

Temperature (K)	301	313	323	333
K_L	1.0622	0.95647	0.93072	0.91746
ΔG°_{ads} (kJ/mol)	-10.202	-10.335	-10.593	-10.881

Table 3 Thermodynamic parameters.

Concentration (g/L)	E_a (kJ/mol)	A	ΔH°_{ads} (kJ/mol)	ΔS°_{ads} (J/mol K)
Blank	32.882	63.688	30.252	-219.21
0.2	30.438	15.596	27.821	-230.93
0.4	30.088	12.379	27.457	-232.84
0.6	31.227	16.184	28.606	-230.62
0.8	31.261	11.473	28.644	-233.48
1.0	34.054	29.636	31.440	-225.59

The positive values of E_A (Table 3) for inhibited solutions (0.2 g/L-0.8 g/L) are lower than those of the uninhibited solution. In contrast, those of the 1.0 g/L inhibited solution are higher than those of the uninhibited solution. At values less than 40 kJ mol^{-1}, the calculated activation energies, E_A, for the adsorption on mild steel in 1.0 M NaOH imply a physisorption process, which means weak electrostatic interaction [15, 26].

Positive values of ΔH°_{ads} ranging between 5 and 40 kJ/mol, indicate an endothermic adsorption process and this implies that the adsorption process is favoured at low temperatures [27]. The negative values of ΔS°_{ads} signifies that adsorption of the extract (inhibitor) onto mild steel surface was orderly. The adsorption mechanism as observed in this study is best described as a physisorption process that involves weak electrostatic intermolecular van der Waals interactions between the molecules of inhibitor and the surface of mild steel [25, 28].

3.4 Electrochemical Investigation

Electrochemical investigations in corrosion experiments enable the prediction of the lifespan of mild steel, the diagnosis of failure nodes, the optimization of mild steel composition, the interaction of inhibitor with metal surface, as well as provision of a mechanistic explanation of corrosion data [29, 30]. The electrochemical impedance spectroscopy (EIS) data are presented in Figure 6 (Nyquist plots, Randle circuit used to fit the EIS data, and Bode plots) and Table 4. Electrochemical impedance spectroscopy, *via* Nyquist analysis, is a non-destructive technique used to determine corrosion mechanisms and rates as well as to evaluate inhibitors' performance and efficiency. The Nyquist plots (Figure 6A) exhibited nearly linear behavior rather than semicircles, which may be attributed to a non-ideal capacitor arising from surface roughness, electrode porosity, or non-uniform current distribution [31]. These factors may lead to the formation of a protective layer of corrosion products, which causes slow diffusion control on the mild steel surface [32]. The Bode plots (Figure 6C) appeared as imperfect sinusoids because of the following reasons: roughness of the mild steel surface; inconsistent build-up of charges at the metal-inhibitor interface as a result of frequency dispersion; or the surface of the mild steel was non-linear or non-stationary [33].

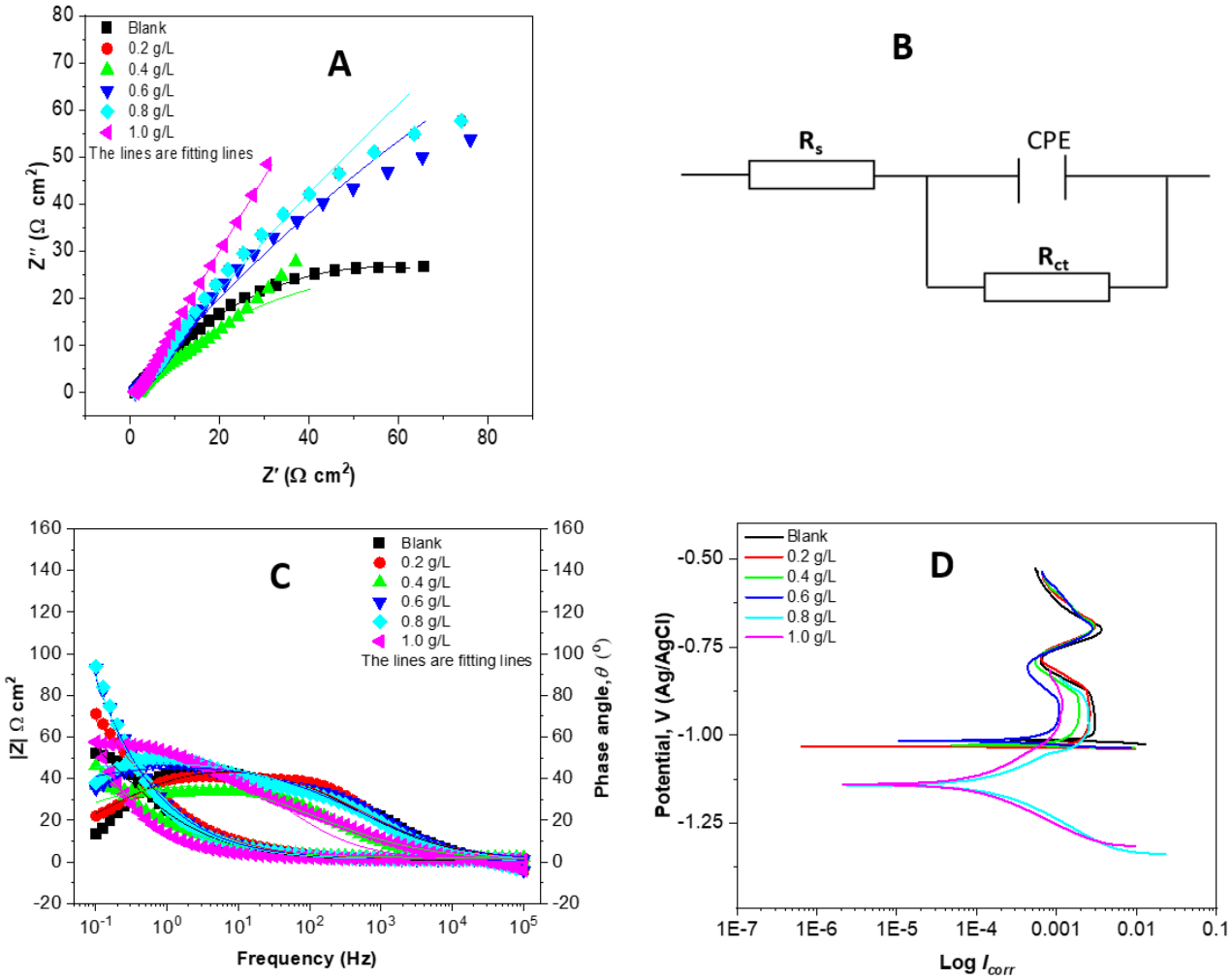

Figure 6 Nyquist plots (A), Randle circuit for fitting the EIS data (B), Bode plots (C), and Tafel plots (D).

Table 4 EIS parameters.

Concentration (g/L)	R_s (Ω cm^2)	R_{ct} (Ω cm^2)	Y_o (×10^{-4} s^n/Ω cm^2)	n	C_{dl} (μF cm^2)	IE_{EIS} (%)
Blank	0.88050	88.469	123.23	0.57449	26.416	-
0.2	1.0772	111.21	98.004	0.56898	19.518	11.409
0.4	1.8529	116.12	198.29	0.50555	16.919	15.155
0.6	1.0040	513.17	129.96	0.54269	18.216	80.801
0.8	1.0555	949.23	137.35	0.55556	20.115	89.621
1.0	1.3095	37000	234.74	0.65135	14.470	97.337

The impedance spectra were analysed, and EIS parameters (R_s, R_{ct}, Y_o, n *and* C_{dl} representing single charge resistance, charge transfer resistance, admittance magnitude, phase shift relating to the surface homogeneity, and double-layer capacitance, respectively) obtained are summarised in Table 4. The R_{ct} value of the uninhibited solution is the lowest, and the R_{ct} value increases as the concentration of the inhibitor increases. The observation, which later translates to an increase in IE_{EIS} %, is a result of the formation of a protective film on the mild steel surface that increased the resistance of the metal to charge transfer [15]. The extreme increase in value of R_{ct} with increasing

concentration of African peach leaf extract signifies resistance of the mild steel against corrosion with near-total efficiency in the system, that is, active blockage of all corrosion sites from the corrosive medium. Similarly, the values of the double-layer capacitance (C_{dl}) of the uninhibited solutions are higher than those of the inhibited solutions. This observation is connected to the increase in the thickness of the adsorbed layer of inhibitor molecules on the surface of the metal, which ultimately causes faster displacement of water molecules and hydrogen ions from the surface of the metal [34].

Tafel plots (polarisation curves) are presented in Figure 6D, while the Tafel parameters are summarised in Table 5. It is evident from the table that corrosion rate (CR_{PDP}) decreases while inhibition efficiency (IE_{PDP} %) increases as the concentration of the inhibitor in the solution increases; this is due to adsorption of inhibitor molecules on the mild steel surface that increases surface coverage and formation of a protective barrier that blocks active corrosion sites [35]. The I_{corr} values in the table decrease as the concentration of inhibitor molecules in the solution increases, which is attributed to an increasing number of inhibitor molecules that reduce the dissolution of mild steel in the alkaline solution [36]. The anomalous phenomenon occurring in the range of -0.5 to -0.9 eV on the Tafel plot (Figure 6D) often results from the formation of surface bubble or diffusion-controlled adsorption mechanism [37], which were similarly observed in the Nyquist (Figure 6A) and Bode (Figure 6C) plots. Although the same experimental conditions were used for EIS and PDP, the inhibition efficiencies obtained by the two techniques differ. This is because the techniques used different electrochemical processes, signal perturbations, mathematical models, and measurement timeframes to evaluate the corrosive medium. Electrochemical impedance spectroscopy evaluates the charge transfer resistance under the steady-state conditions, but PDP evaluates cathodic and anodic polarisation behaviors under dynamic potential scanning.

Table 5 Potentiodynamic polarisation parameters.

Concentration (g/L)	E_{corr} (mV)	I_{corr} (µA/cm^2)	β_a (mV/dec)	β_c (mV/dec)	CR_{PDP} (mm/y)	IE_{PDP} (%)
Blank	-1011.8	1861.1	62.200	16.650	21.588	-
0.2	-1032.7	642.77	27.050	4.5300	7.4561	65.463
0.4	-1029.8	637.25	63.700	8.3700	7.3921	65.759
0.6	-1017.3	185.41	32.860	13.800	2.1510	90.038
0.8	-1141.1	91.317	89.350	82.020	1.0593	95.093
1.0	-1135.0	47.433	64.570	81.590	0.55020	97.451

3.5 Surface Characteristics

The FTIR analysis was carried out to elucidate the functional groups present in the samples, as shown in Figure 7. The FTIR spectra of the extract and mild steel after immersion in inhibited solution (1.0 M NaOH + 1.0 g/L of extract + mild steel) are similar—only showing slight band variations, which could be as a result of interaction of mild steel with the extract solution. The FTIR spectrum of the mild steel shows only a few FTIR bands. The peak at *ca.* 3331 cm^{-1} is assigned to O–H (broad stretching vibration); the bands around 2927 cm^{-1} and 2858 cm^{-1} are assigned to asymmetric stretching of methylene –CH_2– groups (C–H asymmetric stretching vibration), 1700 cm^{-1} and 1650 cm^{-1} are linked to C=O; 1370 cm^{-1} is for CH_3, C–O stretching vibration (aliphatic alcohols, ethers, etc.) is visible at 1020 cm^{-1} while 610 cm^{-1} is linked to C–H bending vibration of an alkyne.

The peak around 1510 cm^{-1} is assigned to NO_2, while the band at 592 cm^{-1} in mild steel FTIR is assigned to Fe–O.

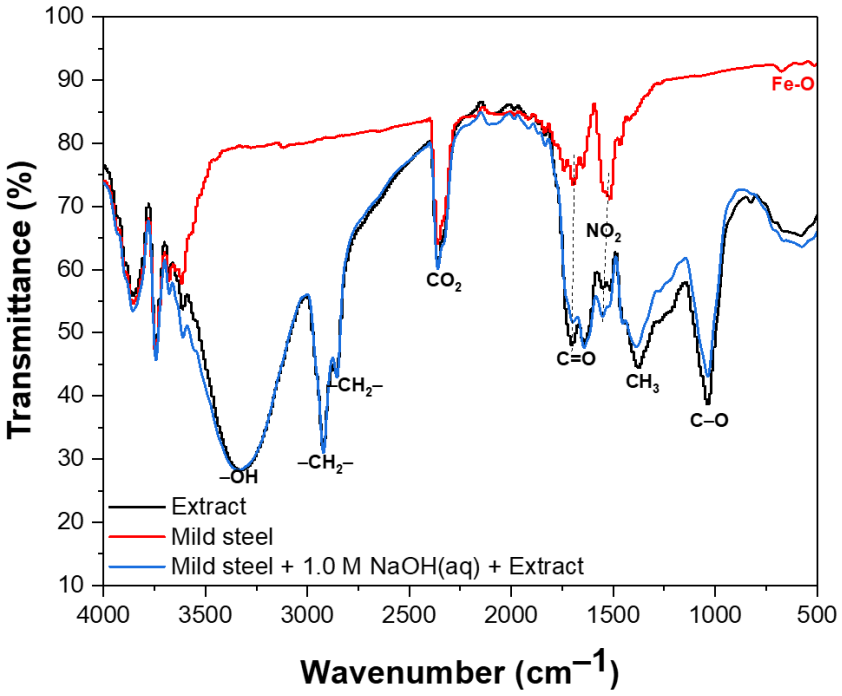

Figure 7 FTIR spectra of the extract, mild steel, and extract + 1.0 M NaOH + mild steel.

The SEM images show the surfaces of the extract (Figure 8A), bare mild steel (Figure 8B), and mild steel after immersion in inhibited solution (Figure 8C). The corresponding EDX spectra that show the relative surface elemental composition are presented in Figure 9. The SEM image of the extract (Figure 8A) shows a smooth, compact surface. The SEM images of the mild steel before immersion (Figure 8B) and after immersion in the inhibited solution (Figure 8C) differ markedly; before immersion in the inhibitor solution, the mild steel surface was rough. However, after immersion in the inhibited solution, the SEM image of the mild steel appears slightly smoother and more compact due to the protective film formed by its inhibitor molecules on its surface. The homogeneous morphology in Figure 8C confirms adsorption of extract molecules on the surface of mild steel, thereby minimizing corrosive attack and enhancing surface protection. The comparison of the EDX spectra of the mild steel and mild steel after immersion in an inhibited solution showed that Fe is still relatively present after corrosion tests. These surface characteristics data agreed closely with the electrochemical data. The reduction in corrosion current density (I_{corr}) and the increase in IE_{PDP} % observed in polarisation studies, as well as the increased R_{ct} from EIS measurements, indicate acceptable corrosion inhibition performance of the African peach extract. The improved surface features of mild steel as observed in the SEM image and the presence of Fe after immersion, as inhibited by EDX analysis, support the conclusion that the African peach extract, as a corrosion inhibitor, protects the mild steel from dissolution by blocking active corrosion sites responsible for the corrosion process [15, 38].

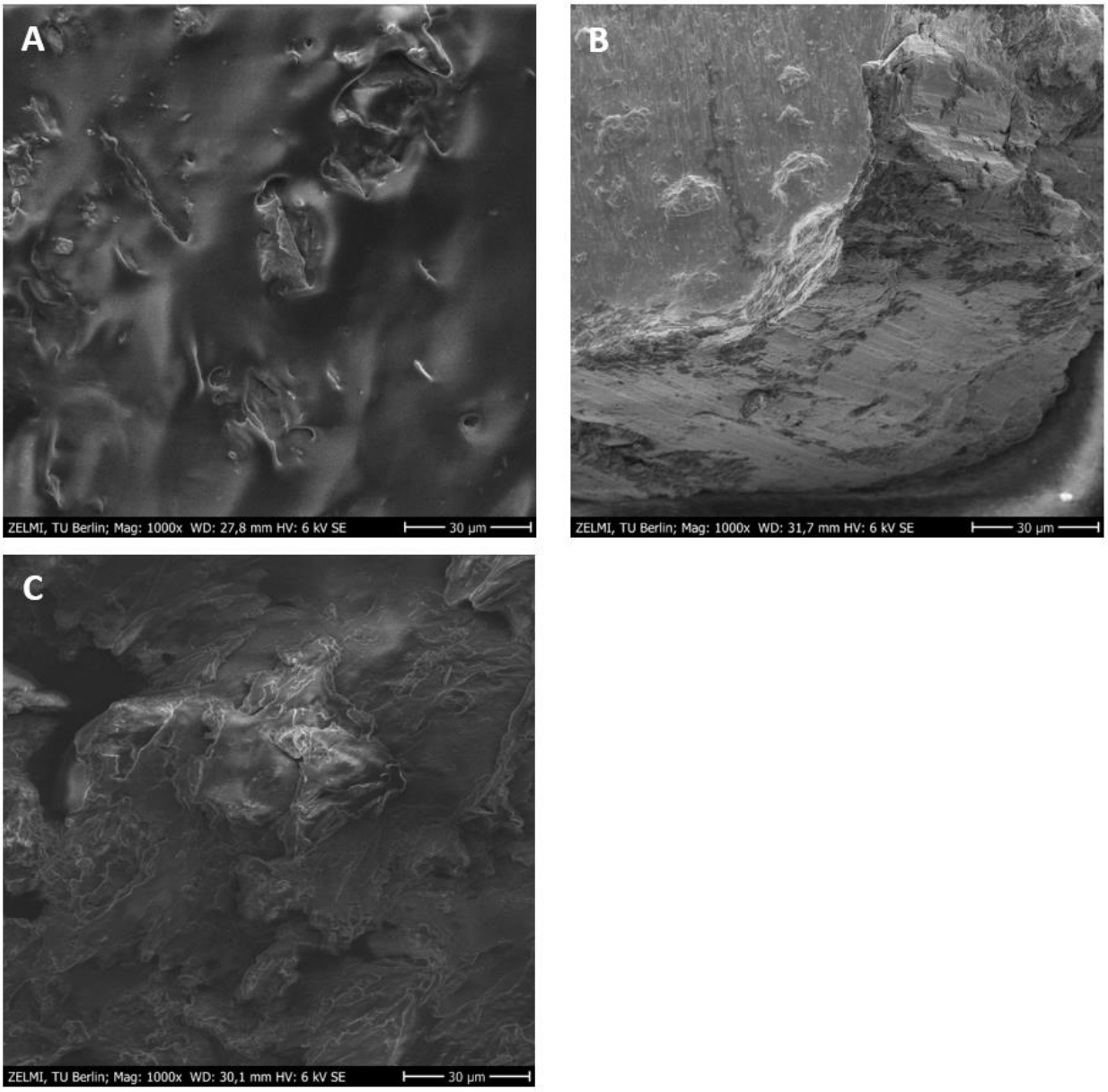

Figure 8 Scanning electron micrographs of the extract (A), mild steel (B), and extract + 1.0 M NaOH + mild steel (C).

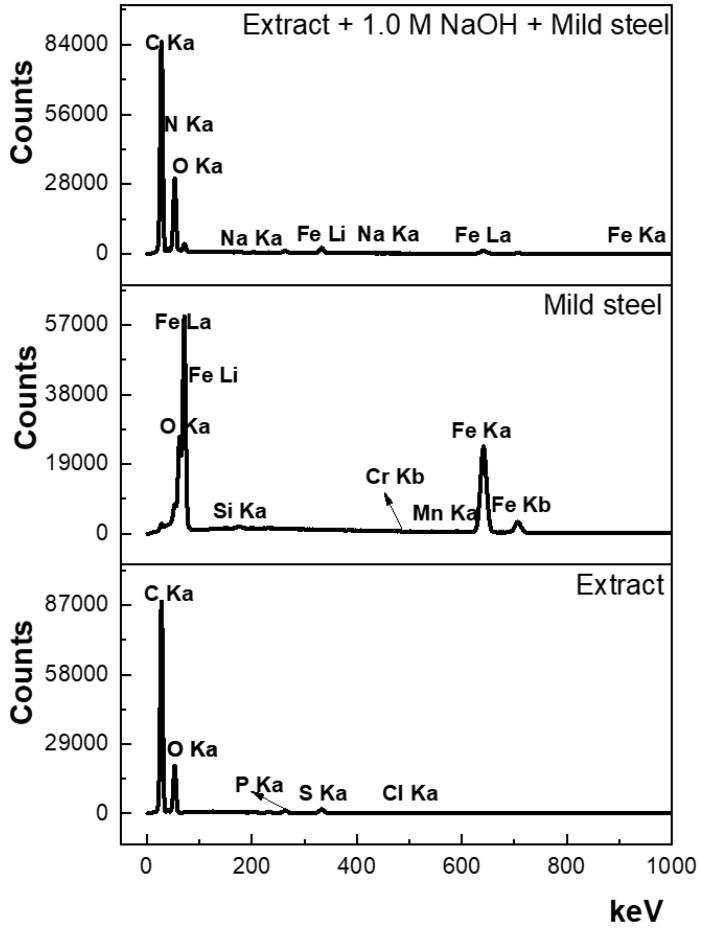

Figure 9 EDX spectra of the extract, mild steel, and extract + 1.0 M NaOH + mild steel.

4. Conclusion

This article reports the usage of *Nauclea latifolia* (African peach) leaves extract as a corrosion inhibitor of mild steel in an alkaline environment (1.0 M NaOH). The data reveal that the extract functions as an effective, environmentally benign corrosion inhibitor for mild steel in 1.0 M NaOH solution. Gravimetric results revealed a gradual decrease in corrosion rate with increasing inhibitor concentration, accompanied by a pronounced improvement in inhibition efficiency, indicating adequate surface coverage by the extract constituents. These deductions are supported by the values of the thermodynamic and kinetic parameters obtained from the equitation after confirmation that the adsorption of African peach extract on mild steel followed the Langmuir isotherm (monolayer on homogenous surface). Electrochemical measurements further corroborated these findings, as evidenced by the reduction in corrosion current density (I_{corr}) and the significant increase in charge transfer resistance (R_{ct}), confirming the formation of a protective adsorbed film of African peach extract on the metal surface. Additionally, surface characterization by SEM-EDX analysis supported these observations, showing improved surface morphology and altered elemental composition in the presence of the inhibitor. The African peach leaf extract can be utilized as a promising alternative material to mitigate corrosion of mild steel in 1.0 M NaOH.

Author Contributions

Matthew A. Adebayo: Data analysis, result presentation, supervision, writing - original draft, and revision; O'Seun Odewale: Data collection, data analysis, investigation, methodology and revision; Olabisi A. Ajayi: Data collection, and methodology.

Competing Interests

The authors declared that there are no competing interests.

AI-Assisted Technologies Statement

The authors declare that this article was prepared without the use of generative AI technologies.

References

1. Umoren SA, Solomon MM, Obot IB, Suleiman RK. A critical review on the recent studies on plant biomaterials as corrosion inhibitors for industrial metals. J Ind Eng Chem. 2019; 76: 91-115.
2. Koch G, Varney J, Thompson N, Moghissi O, Gould M, Payer J. International measures of prevention, application, and economics of corrosion technologies study [Internet]. Houston, TX: NACE International; 2016. Available from: http://impact.nace.org/documents/Nace-International-Report.pdf.
3. Adebayo MA, Aigbogun JA, Oluwafemi KA, Oderemi YO. Extracts of sweet prayer leaf as corrosion inhibitors of mild steel in acidic medium: Effects of extractants' properties. Sci Rep. 2026; 16: 8939.
4. Xie J, Xi R, Tong C, Yan JB. Mechanical properties of Q235~Q460 mild steels at low temperatures. Constr Build Mater. 2023; 363: 129850.
5. Fontana MG, Greene ND. Corrosion engineering. Columbus, OH: McGraw-hill; 2018.
6. Baitule PK, Victoria SN, Manivannan R. Review on assessment of corrosion of mild steel in alkaline environment by using plant extract. IOP Conf Ser Mater Sci Eng. 2021; 1057: 012012.
7. Rihan RO, Nešić S. Erosion-corrosion of mild steel in hot caustic. Part II: The effect of acid cleaning. Corros Sci. 2006; 48: 2660-2675.
8. Emmanuel JK. Corrosion protection of mild steel in corrosive media, a shift from synthetic to natural corrosion inhibitors: A review. Bull Natl Res Cent. 2024; 48: 26.
9. James AO, Akaranta O. Corrosion inhibition of aluminium in 2M sulphuric acid using acetone extract of red onion skin. Int J Appl Chem Sci Res. 2014; 2: 1-10.
10. Adebayo MA, Akande SO, Olorunfemi AD, Ajayi OO, Orege JI, Daniel EF. Equilibrium and thermodynamic characteristics of the corrosion inhibition of mild steel using sweet prayer leaf extract in alkaline medium. Prog Chem Biochem Res. 2021; 4: 80-91.
11. Abd-El-Nabey BA, Abd-El-Khalek DE, El-Housseiny S, Mohamed ME. Plant extracts as corrosion and scale inhibitors: A review. Int J Corros Scale Inhib. 2020; 9: 1287-1328.
12. Verma C, Ebenso EE, Bahadur I, Quraishi MA. An overview on plant extracts as environmental sustainable and green corrosion inhibitors for metals and alloys in aggressive corrosive media. J Mol Liq. 2018; 266: 577-590.

13. Omogbehin SA, Olasehinde EF, Adebayo MA, Jabar JM. Investigating the inhibition of mild steel corrosion by *Tectona grandis* dye extract in acidic environment: Thermodynamics and adsorption properties. Chem Sci Int J. 2024; 33: 93-109.
14. Shittu GA, Ephraim ME. Antimicrobial properties of *Sacrocephalus latifolius* (Sm.) Bruce. J Med Plants Res. 2014; 8: 1116-1120.
15. Agbaffa BE, Olasehinde EF, Adebayo MA, Oladele EO, Akinjokun AI, Esho IJ. Experimental and theoretical investigations of the corrosion protection of mild steel by methanolic *Triumfetta rhomboidea* J. leaf extract. Sustain Chem Environ. 2025; 11: 100270.
16. Aigbogun JA, Adebayo MA. Green inhibitor from *Thaumatococcus daniellii* Benn for corrosion mitigation of mild steel in 1 M HCl. Curr Res Green Sustain Chem. 2021; 4: 100201.
17. Olasehinde EF, Agbaffa EB, Adebayo MA, Abata EO. Corrosion inhibition of mild steel in 1 M HCl by methanolic *Chromolaena odorata* leaf extract: Experimental and theoretical studies. J Bio Tribo Corros. 2022; 8: 105.
18. Aluko AO, Oke GO. Adsorption and thermodynamic studies of carica *Papaya leaves* extract (yellow) as corrosion inhibitor for mild steel in acidic medium. J Mater Sci Res Rev. 2022; 5: 1-12.
19. Quraishi MA, Singh A, Singh VK, Yadav DK, Singh AK. Green approach to corrosion inhibition of mild steel in hydrochloric acid and sulphuric acid solutions by the extract of *Murraya koenigii* leaves. Mater Chem Phys. 2010; 122: 114-122.
20. Agbaffa BE, Olasehinde EF, Adebayo MA. Corrosion protection of mild-steel in 1 M HCl using nanocomposite from *Triumfetta rhomboidei*. Mater Sci Technol. 2023; 39: 2562-2576.
21. Zhang H, Yan L, Zhu Y, Ai F, Li H, Li Y, et al. The effect of immersion corrosion time on electrochemical corrosion behavior and the corrosion mechanism of EH47 ship steel in seawater. Metals. 2021; 11: 1317.
22. Oguzie EE. Corrosion inhibition of aluminium in acidic and alkaline media by *Sansevieria trifasciata* extract. Corros Sci. 2007; 49: 1527-1539.
23. Raja PB, Sethuraman MG. Natural products as corrosion inhibitor for metals in corrosive media-A review. Mater Lett. 2008; 62: 113-116.
24. Kokalj A. On the use of the Langmuir and other adsorption isotherms in corrosion inhibition. Corros Sci. 2023; 217: 111112.
25. Abed KM, Mohsen OA, Al-Issawi AG, Faraj MW, Al-Shuwaiki NM, Rahman SA, et al. A novel amide corrosion inhibitor derived from waste cooking oil for mild steel in hydrochloric acid. Sci Rep. 2025; 15: 41625.
26. Sahmoune MN. Evaluation of thermodynamic parameters for adsorption of heavy metals by green adsorbents. Environ Chem Lett. 2019; 17: 697-704.
27. Aljamali NM, Khdur R, Alfatlawi IO. Physical and chemical adsorption and its applications. Int J Thermodyn Chem Kinet. 2021; 7: 1-8.
28. Ankwai GE, Kolo AM, Mahmoud AA, Chindo IY, Balogun OO. The use of novel biosynthesized Ag-Cu-Al nanoparticles as corrosion inhibitor on mild steel in 1 M HCl medium. Int Res J Pure Appl Chem. 2025; 26: 62-81.
29. Kelly RG, Scully JR, Shoesmith D, Buchheit RG. Electrochemical techniques in corrosion science and engineering. Boca Raton, FL: CRC Press; 2002.

30. Sheetal, Kundu S, Thakur S, Singh AK, Singh M, Pani B, et al. A review of electrochemical techniques for corrosion monitoring-fundamentals and research updates. Crit Rev Anal Chem. 2025; 55: 161-186.
31. Barsoukov E, Macdonald R. Impedance spectroscopy theory, experiment, and applications. Hoboken, NJ: John Wiley & Sons, Inc.; 2005.
32. Boadu MK, Agyei-Agyemang A, Andoh P, Adam F. Sequential trends in corrosion behaviour of surface-ground aluminium 7075 Thin Plates in 3.5 wt% NaCl solution he potentiodynamic polarization method. MUST J Res Dev. 2025; 6: 12.
33. Ansari KR, Quraishi MA. Bis-Schiff bases of isatin as new and environmentally benign corrosion inhibitor for mild steel. J Ind Eng Chem. 2014; 20: 2819-2829.
34. Doss JR, Shanahan MH, Wohl CJ, Connell JW. Synthesis, characterization and evaluation of urethane co-oligomers containing pendant fluoroalkyl ether groups. Prog Org Coat. 2016; 95: 72-78.
35. Shwetha KM, Praveen BM, Devendra BK. A review on corrosion inhibitors: Types, mechanisms, electrochemical analysis, corrosion rate and efficiency of corrosion inhibitors on mild steel in an acidic environment. Results Surf Interf. 2024; 16: 100258.
36. Abdallah M, Hegazy MA, Alfakeer M, Ahmed H. Adsorption and inhibition performance of the novel cationic Gemini surfactant as a safe corrosion inhibitor for carbon steel in hydrochloric acid. Green Chem Lett Rev. 2018; 11: 457-468.
37. Zhang Q, Yu Y, Li J, Yin C, Tian F, Liu J, et al. Synergistic corrosion inhibition and UV protection via TTA-loaded LDH nanocontainers in epoxy coatings. Coatings. 2025; 15: 505.
38. Akilu A, Abdullahi MS, Aliyu AJ. Exploring the use of plant extracts from leaves, bark, and roots of *Boswelia dalzelia* as corrosion inhibitors on low-carbon steel embedded in concrete as reinforcement when subjected to chloride and acidic environment. Recent Prog Sci Eng. 2026; 2: 005.